ELSEVIER

Journal of Organometallic Chemistry 637–639 (2001) 683–690

Journal of Organometallic Chemistry

www.elsevier.com/locate/jorganchem

Synthetic, electrochemical, and structural studies on heterobimetallic crown thioether complexes with Group 10 metals: the crystal structures of $[Pt(9S3)(dppf)](PF_6)_2 \cdot CH_3NO_2$ and $[Pd(9S3)(dppf)](PF_6)_2 \cdot CH_3NO_2$

Gregory J. Grant [a,*], Shawn M. Carter [a], A. LeBron Russell [a], Ivan M. Poullaos [a], Donald G. VanDerveer [b]

[a] *Department of Chemistry, Dept. 2252, The University of Tennessee at Chattanooga, 615 McCallie Avenue, Chattanooga, TN 37403-2598, USA*
[b] *School of Chemistry and Biochemistry, Georgia Institute of Technology, Atlanta, GA 30332, USA*

Received 20 February 2001; received in revised form 10 April 2001; accepted 29 April 2001

Abstract

The syntheses, electrochemistry, and crystal structures for two new Pt(II) and Pd(II) heteroleptic bimetallic complexes with the crown trithioether 1,4,7-trithiacyclononane (9S3) and the diphosphine ligand, 1,1′-bis(diphenylphosphino)ferrocene (dppf) are reported. Both complexes have the general formula $[M(9S3)(dppf)](PF_6)_2$ (M = Pt or Pd) and exhibit the anticipated structure forming a distorted *cis* square planar array of two sulfur atoms from the 9S3 and two phosphorus atoms. These are, to our knowledge, the first reported examples of dppf transition metal complexes involving a thioether as the ancillary ligand. The dppf ligand functions as a bidentate chelator to a single metal center, and the third 9S3 sulfur atom does interact with the metal ion from a greater distance (Pt–S = 2.8167(8) Å; Pd–S = 2.7916(5) Å) to yield an elongated square pyramidal geometry. The two structures are isomorphous with very similar bond distances and angles. The values for the ^{31}P-NMR chemical shifts (Pt = 15.09 ppm, Pd = −0.47 ppm), the ^{195}Pt-NMR chemical shift for the Pt(II) complex (−4353 ppm) and $^1J(^{195}Pt-^{31}P)$ coupling constants (3511 Hz) are all consistent with a *cis*-MS_2P_2 square planar coordination sphere. The 9S3 ligand is fluxional in solution for both complexes. The electrochemistry of both complexes is dominated by a reversible Fe(II)/Fe(III) couple from the ferrocene moiety ($E_{1/2}$ = +721 mV for Pt(II), +732 mV for Pd(II), both versus Fc/Fc^+).

Keywords: Crown thioethers; Diphosphine ligands; Crystal structures; Electrochemistry

1. Introduction

The past decade has witnessed a remarkable increase in the research of crown thioethers, such as 1,4,7-trithiacyclononane (9S3), in a number of areas, including transition metal complexes, main group compounds, and organometallic complexes [2–8]. An important focus of thioether coordination chemistry has been the platinum group metal ions because of the unusual properties that their complexes demonstrate. Homoleptic thioether complexes with these particular metal ions have been shown to stabilize unique oxidation states (trivalent platinum), to exhibit remarkable electronic spectra featuring d–d visible absorption bands and unusual complex colors (green Pd(II)), and to form exotic coordination geometries (octahedral Rh(I)) [9–17]. For thioether complexes involving Pd(II) and Pt(II), their unusual properties have been shown to be a direct consequence of long distance interactions between the metal center and axial sulfur atoms [18]. In the absence of the metal–sulfur interactions, more typical complex behavior is observed, and the structural characteristics are lacking in Pt(II) or Pd(II) complexes with larger crown thioethers, acyclic thioethers, and mixed donor oxathioethers [19]. These long distance interactions result in unusual complex structures such as elongated square pyramids [$S_4 + S_1$] [10] or elongated

* Corresponding author. Tel.: +1-423-755-4278; fax: +1-423-755-5234.
E-mail address: greg-grant@utc.edu (G.J. Grant).

0022-328X/01/$ - see front matter
PII: S0022-328X(01)00964-0

octahedra [$S_4 + S_2$] [9,11–14]. The nature of the metal–axial sulfur interactions is of considerable theoretical interest, and they have been described in a variety of ways (weak bonds, 'half' bonds, agostic interactions, etc.) [20]. In addition, these types of 9S3 complexes have been highlighted as models for ligand substitution reactions which proceed by associative mechanisms in four-coordinate complexes [21].

The diphosphine ligand 1,1-bis(diphenylphosphino-ferrocene) (dppf) is noted for its excellent chelating ability, and an extensive coordination chemistry has now emerged surrounding this ligand [22–26]. Interest in dppf as a ligand has focused on the structural aspects of its complexation behavior since it displays a variety of coordination modes [22]. Also, the electrochemistry and potential catalytic roles of its complexes are being investigated. Phosphine ligands are known to be effective catalysts, especially chiral diphosphines as asymmetric catalysts [27]. Furthermore, the catalytic activity of diphosphine ligands has been correlated with the bite angle of the chelate ring [28]. As noted above, several homoleptic Pt(II) and Pd(II) complexes with crown thioethers have been structurally characterized, but heteroleptic phosphine-crown thioether complexes remain relatively unexplored [1,29]. Lastly, ^{195}Pt- and ^{31}P-NMR chemical shifts and couplings can provide additional data to probe the interactions between these ligands and the platinum group metals [30].

2. Results and discussion

2.1. Syntheses and spectroscopic data

The two new heteroleptic complexes, [Pt(9S3)(dppf)]-$(PF_6)_2$ and [Pd(9S3)(dppf)]$(PF_6)_2$, are readily prepared by ligand substitution reactions from their dichloro complexes and subsequently isolated as hexafluorophosphate salts. These reactions are illustrated in Scheme 1. For the Pt(II) complex, we have employed [Pt(9S3)Cl_2] as the starting reagent, displacing the two chloride ligands with dppf [31]. A similar reaction using [Pd(9S3)Cl_2] [29,32] can be used to prepare the palladium analog, but yields are lowered by the competing formation of the green–blue *bis* (9S3) complex. We have found the synthesis of this complex to be more efficient beginning with the commercially available [Pd(dppf)Cl_2]·CH_2Cl_2.

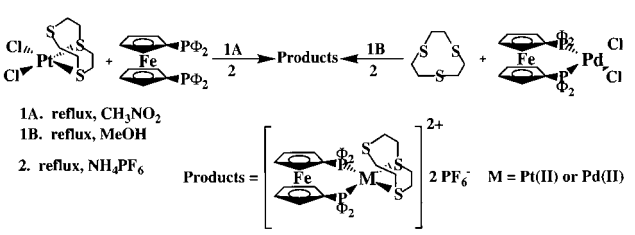

Scheme 1. Synthesis of [M(9S3)(dppf)]$(PF_6)_2$ complexes.

In contrast, we have not been able to prepare the analogous mixed phosphine–thioether Ni(II) complex, $[Ni(9S3)(dppf)]^{2+}$, from [Ni(dppf)]Cl_2] under a variety of experimental conditions [33]. Instead, the only isolated products are the pink complex, $[Ni(9S3)_2]^{2+}$, along with recovered yellow dppf ligand. We suggest that the stereochemical demands of the two ligands may be responsible for the different behavior in the Ni(II) case. The dppf ligand has a relatively large P–M–P bite angle which can be accommodated by Ni(II) more readily in a tetrahedral structure. Indeed, the Cl–Ni–Cl chelate angle in the crystal structure of [Ni(dppf)]Cl_2] is 124.5(1)° [26]. However, the 9S3 ligand necessarily requires a *cis* square planar coordination to coordinate in a polydentate fashion. The Pd(II) and Pt(II) ions can provide a better electronic match and are more readily complexed by the dppf in a distorted square planar structure (see below). The smaller Ni(II) ion cannot do this. The difficulties of synthesizing heteroleptic Ni(II) complexes of 9S3 with sterically crowded diphosphine ligands have been reported previously [34]. Our results demonstrate that the tendency for the formation of bis(9S3) complexes is favored to a greater extent for 3d transition metals than for later ones.

The presence of the 9S3 and dppf ligands as well as uncoordinated hexafluorophosphate is confirmed via infrared spectroscopy, and the elemental analyses are consistent with the reported complex stoichiometries containing one nitromethane solvent per complex. The electronic spectra for the complexes are dominated by the dppf moiety. In the Pt(II) complexes, two bands are observed with the long wavelength band assigned as the $d\pi$ (Fe) $\rightarrow \pi^*$ (Cp) MLCT band and the short wavelength band as the $\pi \rightarrow \pi^*$ transition of the phenyl group of the dppf ligand. The MLCT band is blue-shifted relative to the free dppf ligand (442 nm vs. 411 nm) as observed in related dppf complexes of Pt(II) [25]. For the Pd(II) complex, the MLCT band has shifted more into the visible and become more intense, resulting in a very deeply colored material. This complex also shows a third band near 360 nm, possibly due to a $d\pi$ (Pd) $\rightarrow \pi^*$ (dppf) MLCT, and this transition may account for the shoulder near 310 nm in the Pt complex.

The ^{1}H- and ^{13}C-NMR spectra of both complexes show the correct number of peaks, splittings, and intensities associated with the three components; four phenyl rings from the dppf ligand, two Cp rings from the dppf ligand, and the 9S3 ligand. The 9S3 region of the proton NMR spectrum appears as a characteristic AA′BB′ splitting pattern of the twelve methylene protons of the 9S3 ligand [1,21,29]. In addition, ^{13}C DEPT experiments confirm all carbon connectivity. In both

Table 1
Crystallographic data for $[Pt(9S3)(dppf)](PF_6)_2 \cdot CH_3NO_2$ and $[Pd(9S3)(dppf)](PF_6)_2 \cdot CH_3NO_2$

	$[Pt(9S3)(dppf)](PF_6)_2 \cdot CH_3NO_2$	$[Pd(9S3)(dppf)](PF_6)_2 \cdot CH_3NO_2$
Empirical formula	$C_{41}H_{43}FeF_{12}NO_2P_4PtS_3$	$C_{41}H_{43}FeF_{12}NO_2P_4PdS_3$
Formula weight	1280.80	1192.07
Space group	$P2_1/c$	$P2_1/c$
Unit cell dimensions		
a (Å)	10.9741(2)	10.9537(6)
b (Å)	14.5797(2)	14.5514(7)
c (Å)	28.7538(4)	28.7539(14)
β (°)	95.84(2)	95.7760(10)
V (Å^3)	4576.74(12)	4559.9(4)
Z	4	4
Radiation (λ, Å)	0.71073	0.71073
ρ_{calc} (g cm^{-3})	1.713	1.736
μ (mm^{-1})	3.733	1.078
T (K)	193(2)	173(2)
Reflections collected	28628	28091
R [a]	0.0324	0.0305
R_w [b]	0.0630	0.0606
Goodness-of-fit on F^2	1.088	1.077

[a] $R = \Sigma| |F_o|-|F_c| | \Sigma |F_o|$.
[b] $R_w = [\Sigma w(|F_o|-|F_c|)^2/\Sigma w(F_o)]^{1/2}$.

Table 2
Selected interatomic bond length (Å) and bond angles (°) for $[Pt(9S3)(dppf)](PF_6)_2 \cdot CH_3NO_2$ and $[Pd(9S3)(dppf)](PF_6)_2 \cdot CH_3NO_2$. M = Pt(II) and Pd(II)

	$[Pt(9S3)(dppf)](PF_6)$	$[Pd(9S3)(dppf)](PF_6)_2$
Bond length		
M–S_{eq}	2.3486(7), 2.4101(7)	2.3534(5), 2.4358(5)
M–S_{axial}	2.8167(8)	2.7916(5)
M–P_{eq}	2.3103(7), 2.3135(7)	2.3213(5), 2.3388(5)
M–Fe	4.092(7)	4.272(5)
P–P	3.471(7)	3.482(5)
Bond angles		
S_{eq}–M–S_{eq}	86.65(2)	86.404(16)
P(1)–M–P(2)	97.28(2)	96.712(16)
P(1)–Fe–P(2)	65.70(2)	62.710(16)
P(1)–M–S_{eq}	175.34(2), 90.87(2)	175.384(17), 91.437(16)
P(2)–M–S_{eq}	160.48(2), 83.90(2)	159.940(17), 84.078 (16)
S_{eq}–M–S_{axial}	81.23(2), 84.80(2)	85.136(16), 81.345(16)

complexes the 9S3 ligand is fluxional resulting in a single resonance for the six equivalent carbons. This phenomena has been observed in every known 9S3 complex of Pt(II) and Pd(II) and contrasts their solid state structures [1,10,35]. The fluxionality arises from the rapid intramolecular exchange of three sulfur atoms of the 9S3 ligands (1,4-metallotropic shift) [21,31,36]. The carbon atom adjacent to the phosphorus in both the Cp and phenyl rings shows the anticipated ^1J couplings. In both complexes, the *ortho* and *meta* carbon atoms of the phenyl rings in the dppf show a complex splitting pattern, possibly arising from longer range $^{13}C-^{31}P$ coupling.

For both cases, the ^{31}P-NMR spectrum consists of a sharp singlet showing the magnetic equivalence of the two phosphorus atoms of the dppf moiety. These resonances occur at +15.09 ppm for the Pt complex and +4.07 ppm for the Pd complex. The ^{31}P-NMR resonance in the Pt complex is shifted downfield relative to the peaks observed in a related series of Pt(II)/dppf complexes with polypyridyl ligands which fall in the 2.27–4.43 ppm range [24]. This may reflect the differences in donor/acceptor characteristics between the two types of ligands or possibly the long distance interaction of the third sulfur from the 9S3. The ^{31}P-NMR chemical shift in $[Pt(9S3)(dppf)]^{2+}$ is near the value we have observed for $[Pt(9S3)(PPh_3)_2]^{2+}$ (12.0 ppm), but upfield from the resonance observed in $[Pt(9S3)(dppm)]^{2+}$ (51.0 ppm) [1].

Due to the presence of both NMR active and non-active Pt centers, a doublet of ^{195}Pt satellites appears in the ^{31}P-NMR spectrum of the Pt complex. The $^1J(^{195}Pt-^{31}P)$ coupling constants occur at 3511 Hz, a relatively large value for 9S3/diphosphine complexes which may be a consequence of the large P–Pt–P chelate bite angle in the dppf case. We have previously noted correlations between $^1J(^{195}Pt-^{31}P)$ coupling constants and the P–Pt–P chelate bite angle [1], and selectivity of diphosphine catalysts in such reactions as hydroformylation and cross coupling has been related to their P–M–P bite angles [28]. The ^{195}Pt-NMR spectrum for $[Pt(9S3)(dppf)]^{2+}$ shows the anticipated triplet splitting pattern (Pt coupled to two ^{31}P donors) centered at −4353 ppm. As observed in the ^{31}P-NMR spectra, this chemical shift is close to the value we previously observed for $[Pt(9S3)(PPh_3)_2]^{2+}$ (−4399 ppm). However, it is considerably downfield from the ^{195}Pt-NMR chemical shift of $[Pt(9S3)(dppm)]^{2+}$ (−4601 ppm). This could reflect differences in the donor/acceptor properties of dppf and dppm (the dppf ligand will be a poorer Lewis base), but steric constraints cannot be eliminated.

2.2. Structural studies

A summary of the crystallographic data for $[Pt(9S3)(dppf)](PF_6)_2 \cdot CH_3NO_2$ and $[Pd(9S3)(dppf)](PF_6)_2 \cdot CH_3NO_2$ appears in Table 1. Key bond lengths and bond angles for the two structures are given in Table 2, and Fig. 1 illustrates an ORTEP perspective of the Pt complex. Also, Fig. 2 shows key angles and distances for each coordination sphere. The two complexes are isomorphous, crystallizing in the same space group, $P2_1/c$, with remarkably similar unit cell parameters, bond distances, and bond angles. The divalent metal center is surrounded by a distorted square planar

array of two *cis* coordinating sulfur atoms and two phosphorus atoms with the metal atom located slightly above the mean square plane of the four ligating atoms and raised towards the axial sulfur donor atom. The dppf ligand coordinates as a bidentate chelator in an η^2 fashion, by far its most common coordination mode out of several possibilities [22]. The 9S3 ligand adopts an *endodentate* conformation, resulting in an axial interaction between the metal center and the third sulfur, but at a greater distance than the two equatorial sulfurs. The geometry for the two complexes is best described as an elongated square pyramid with $S_2P_2 + S_1$ coordination. Similar molecular shapes have also been observed for heteroleptic Pt(II) and Pd(II) complexes of 9S3 with other diphosphine ligands [1,29].

Dppf complexes of Group 10 metals are by far the most commonly studied family with over 40 crystal structures having been reported [22,37]. However, to our knowledge, the two complexes described here not only constitute the first examples of structurally characterized Group 10 dppf complexes with thioether ligands, but also the first transition metal complexes containing dppf and thioethers. In the Pt(II) complex, the two Pt–P distances are 2.3103(7) and 2.3135(7) Å, somewhat longer than those in the related dppm and $2 \times PPh_3$ complexes [1]. The two equatorial Pt–S bond distances are 2.386(7) and 2.4101(7) Å, with the shorter Pt–S bond *trans* to the shorter Pt–P bond. This observation holds true for all known 9S3/diphosphine complexes involving Group 10 metal ions. The axial sulfur does indeed exhibit an interaction with the Pt(II) center and approaches it at 2.8167(8) Å [38]. This is over 0.15 Å longer than the axial interaction observed for the 9S3/dppm or $9S3/2 \times PPh_3$ complexes ($Pt–S_{axial}$; dppm = 2.666(6) Å, $2 \times PPh_3$ = 2.638(3) Å) [1]. The Pt(II) ion is raised by 0.2214(4) Å above the mean square plane and directed towards the axial sulfur donor. The four atoms in the equatorial plane have an average displacement of 0.1349 Å. Note that the Fe–M distance in either dppf complex is too large (> 4.0 Å) to allow any metal–metal interactions to take place.

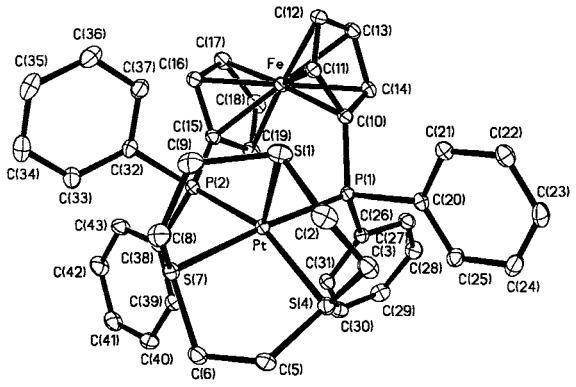

Fig. 1. ORTEP perspective of $[Pt(9S3)(dppf)](PF_6)_2 \cdot CH_3NO_2$.

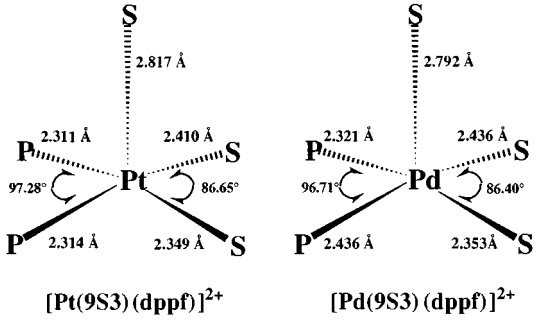

Fig. 2. Coordination spheres of $[M(9S3)(dppf)]^{2+}$ complexes.

The P–Pt–P chelate bite angle is 97.28(2)°, large for a square planar complex, and larger than the other reported Pt 9S3/diphosphine complexes (dppm = 72.70(2)°, $2 \times PPh_3$ = 95.58(7)°). Nevertheless, it is one of the smallest P–M–P angles observed in any Group 10 structure of the dppf ligand [22]. Furthermore, the Pd(II) complex (see below) has an even smaller diphosphine bite angle. The presence of 9S3 as the ancillary ligand could be responsible for these unusually small P–M–P angles within the dppf chelate. The S–Pt–S angle is depressed from 90°, down to 86.65(2)°. There is a reciprocal relationship in these types of complexes between the P–M–P chelate angle and the S–M–S chelate angle so that as one angle opens up, the other compresses. The sum of the bond angles surrounding the platinum center is 358.70(2)°, showing a little distortion from an ideal square-planar geometry. The two Cp rings in the dppf ligand are in the synclinal staggered formation, the most commonly observed conformation for dppf complexes, with a characteristic P–Fe–P angle of 65.70(2)° and a common value of the structural parameter, τ, of 42.24° [22,39]. Consistent with these data, the dihedral angle for C10–P1–P2–C15 is 36.8(2)°, close to the ideal value of 36° for the staggered conformation. The two Cp rings are almost parallel, with a mean dihedral angle of only 2.53°.

For the Pd(II) complex, the two Pd–P distances are 2.3213(5) and 2.3388(5) Å, again longer than those in the related dppm and $2 \times PPh_3$ complexes [26]. The two equatorial Pt–S bond distances are 2.3534(5) and 2.4358(5) Å with the shorter M–S bond *trans* to the shorter M–P bond. As with platinum, the axial sulfur shows an interaction with the Pd(II) center and approaches it at 2.7916(85) Å, forming an *endodentate* conformation of the 9S3 ligand. The length is over 0.15 Å longer than the axial interaction observed for the Pd(II)/9S3 complex with dppm (2.698(3) Å), but a closer approach than the $2 \times PPh_3$ complex (2.877(3) Å) [1]. As seen from the bond angles in Table 2, the axial sulfur (S1) lies away from the dppf ligand and bends slightly towards S4, the same orientation of the 9S3 that is also seen in the Pt(II) complex. The Pd(II) ion sits slightly above (0.2303(3) Å) the mean square plane,

again inclined towards the axial sulfur atom. The four atoms in the equatorial plane have an average displacement of 0.1416 Å. The P–Pd–P chelate bite angle is 96.712(16)°, and this value is the smallest yet observed in any structure of Group 10/dppf complex [22]. The S–Pd–S angle is again depressed from 90°, down to 86.404(16)°. The sum of the bond angles around the Pd(II) is 358.63(2)°, similar to the Pt(II) value and again showing a little distortion from an ideal square-planar geometry. The two Cp rings in the dppf ligand exhibit the common synclinal staggered formation with a P–Fe–P angle of 62.710(16)° and a τ value of 41.81°. The C10–P1–P2–C15 dihedral angles are again close to 36 at 32.2(2)°. In this structure, the two Cp rings are almost parallel, with a mean dihedral angle of only 2.37°.

2.3. Electrochemical studies

The electrochemistry for both complexes is dominated by a single reversible oxidation wave which is assigned to the Fe(II)/Fe(III) couple of the ferrocene moiety in the dppf ligand. The couple occurs with an $E_{1/2}$ value of $+721$ mV versus Fc/Fc^+ for the Pt(II) complex and with a similar value of $+732$ mV versus Fc/Fc^+ in the palladium case. The reversibility of the oxidation is demonstrated in two ways. First, the peak-to-peak separation for the wave in both complexes is near 70 mV, close to the value we obtain in the voltammograms of ferrocene and dppf, both of which are reversible. Second, the i_{pa}/i_{pc} ratio for the Fe(II)/Fe(III) couple in both dppf complexes is very nearly one. We would like to note that the presence of the ferrocene reference does slightly affect the reversibility of the oxidation for the palladium complex, possibly due to an interaction with the ferrocenium ion. For the Fe(II)/Fe(III) couple in the two complexes, there is an anodic shift of over 500 mV compared to the uncomplexed dppf ligand. Thus, the Fe(II) center is harder to oxidize in both complexes, a result of the redistribution of electron density due to the second dicationic metal center being present. Also, the couple in the Pt complex is more anodic (over 400 mV) than for related dppf complexes with anionic ligands such as chloride which are better ligand donors and are more effective at neutralizing the positive charge of the platinum center [25]. In addition, the oxidation in the two 9S3 complexes is a fully reversible one whereas the related examples report irreversible or quasi-reversible behavior.

The Pt(II) complex shows one irreversible reduction wave at -1454 mV versus Fc/Fc^+. This is a one electron process and is assigned as the Pt(II)/Pt(I) couple. Both the oxidative and reductive electrochemical behavior of the complex are quite similar to the reported Pt(II) dppf complexes involving neutral polypyridyl ligands [24]. Our electrochemical results may indicate that crown thioethers such as 9S3 have similar donor/acceptor properties to polypyridines. In contrast, the Pd(II) complex shows two irreversible reductions. The first is well defined and occurs at -880 mV versus Fc/Fc^+. This is assigned as a Pd(II)/Pd(I) couple, similar to those observed in related Pd(II) heteroleptic thioether/phosphine complexes [29]. Also, a second broad, poorly defined irreversible reduction wave is observed at -1476 mV versus Fc/Fc^+, possibly a Pd(I)/Pd(0) couple although an iron-centered reduction cannot be eliminated. All reductions waves, however, appear to be due to the presence of the second metal center since none are present in voltammograms of the dppf ligand.

3. Conclusions

Two new Pt(II) and Pd(II) heteroleptic bimetallic complexes with the crown trithioether, 1,4,7-trithiacyclononane (9S3) and the diphosphine ligand, 1,1′-bis(diphenylphosphino)ferrocene (dppf) were readily prepared. In contrast, the analogous Ni(II) complex could not be prepared, probably due to stereochemical demands of the two ligands. Both complexes have the general formula $[M(9S3)(dppf)](PF_6)_2$ (M = Pt or Pd) and exhibit solid state structures best described as $S_2P_2 + S_1$ coordination. To our knowledge, these are the first structurally characterized transition metal complexes of dppf involving a thioether as the ancillary ligand. The dppf ligand functions as an η^2 bidentate chelator to a single metal center, and two of the three sulfur donors from the 9S3 complete the equatorial square planar environment. The third 9S3 sulfur atom does interact with the metal ion from a greater distance (Pt–S = 2.8167(8) Å, Pd–S = 2.7916(5) Å) in an axial fashion to yield an elongated square pyramidal geometry. The two structures are isomorphous with very similar bond distances and angles, and the P–Fe–P angles are the smallest yet observed for Group10 dppf complexes. The values for the ^{31}P- and ^{195}Pt-NMR chemical shifts and $^1J(^{195}Pt–^{31}P)$ coupling constants are consistent with a *cis*-MS_2P_2 square planar coordination sphere and follow trends previously observed for other diphosphine complexes. The 9S3 ligand is fluxional in solution for both complexes. The electrochemistry of the two complexes is dominated by a reversible Fe(II)/Fe(III) couple from the ferrocene moiety ($E_{1/2} = +721$ mV for Pt(II), $+732$ mV for Pd(II), both vs. Fc/Fc^+). This value shows an anodic shift compared to the uncomplexed dppf ligand and dppf complexes with anionic ligands.

4. Experimental

4.1. Materials

Starting reagents $[Pd(dppf)Cl_2]\cdot CH_2Cl_2$ and 9S3 were purchased from Aldrich chemical company and used as received. All other compounds and solvents were also purchased from Aldrich chemical company and used as received except for the complex $[Pt(9S3)Cl_2]$ [31] which was prepared by the literature methods.

4.2. Measurements

Elemental analyses were performed by Atlantic Microlab, Inc., of Atlanta, GA. Fourier transform infrared spectra were obtained using a Galaxy FTIR 5000 spectrophotometer equipped with an ATR accessory, and UV–vis spectra were obtained on a Varian DMS 200 UV–vis spectrophotometer. ^{13}C- and ^{1}H-NMR spectra were recorded on a Varian Gemini 300 NMR spectrometer using CD_3NO_2 for both the deuterium lock and reference. All observed carbon resonance connectivities were confirmed via DEPT (Distortionless Enhancement by Polarization Transfer) experiments. ^{195}Pt-NMR spectra were recorded near 64.208 MHz using aqueous solutions of $[PtCl_6]^{2-}$ (0 ppm) as an external reference and delay time of 0.01 s. Referencing was verified versus authentic samples of $[PtCl_4]^{2-}$ which was found to have a chemical shift at -1626 ppm, in agreement with the reported value of -1624 ppm [30]. ^{31}P-NMR referencing was done using phosphoric acid (0 ppm) as an external standard. A Biological Analytical Supply CV-50W Potentiostat was used for all electrochemical measurements. The supporting electrolyte was 0.05 M $(Bu)_4NBF_4$ in CH_3CN, and sample concentrations were 0.1 mM (Pt complex) and 0.3 mM (Pd complex). All voltammograms were recorded at a scan rate of 100 mV s^{-1}. The standard three-electrode configuration was as follows: glassy carbon working electrode, Pt-wire auxiliary electrode, and Ag | AgCl reference electrode. All potentials were internally referenced against the Fc/Fc^+ couple. Magnetic susceptibility measurements on solid samples were obtained using a Johnson–Matthey magnetic susceptibility balance at ambient temperatures, and standard diamagnetic correction factors were employed.

4.3. Syntheses

4.3.1. Preparation of $[Pt(9S3)(dppf)](PF_6)_2\cdot CH_3NO_2$

A mixture of $[Pt(9S3)Cl_2]$ (93.0 mg, 0.208 mmol) and dppf (0.122 g, 0.220 mmol) was refluxed in 50 ml of CH_3NO_2 for 3 h. The resulting solution was allowed to cool slightly before NH_4PF_6 (75.0 mg, 0.460 mmol) was added, and the mixture was refluxed for an additional 30 min. The solution was hot-filtered and concentrated on a rotary evaporator to less than two-thirds its original volume. Dark orange crystals of $[Pt(9S3)(dppf)](PF_6)_2\cdot CH_3NO_2$ (174 mg, 68.8% yield) were obtained by diffusion of ether into the nitromethane concentrate, and these were suitable for X-ray diffraction studies. Anal. Found: C, 38.64; H, 3.37; S, 7.57. Calc. for $C_{41}H_{43}F_{12}NO_2P_4PtFeS_3$: C, 38.38; H, 3.38; S, 7.50%. The electronic absorption spectrum measured in MeCN showed two transitions with the first λ_{max} at 396 nm ($\varepsilon = 539$) and a second with a λ_{max} at 254 nm ($\varepsilon = 19\,600$) with a shoulder at 308 nm ($\varepsilon = 2900$). FTIR (KBr, cm^{-1}): 3067, 3065, 3060, 3057, 2991, 2988, 2983, 2860, 1486, 1242, 1175, 1020, 1010, 842 (s, PF_6^-), 777, 651, 643, 592, 588. ^{1}H-NMR (CD_3NO_2): δ = Ph: multiplets at 7.88 and 7.66 (20H); Cp: singlets at 4.72 (4H) and 4.63 (4H); 9S3: complex AA′BB′ pattern at 2.83 (6H) and 2.45 (6H). $^{13}C\{^{1}H\}$-NMR (CD_3NO_2): δ = Ph: multiplets at 138.0, 135.3, 134.0, 133.2 (24C); Cp: singlets at 79.0 and 78.4 (8C) and a doublet at 69.9 (2C, $^{1}J(^{13}C-^{31}P) = 69$ Hz); 9S3: singlet at 37.4 (6C). $^{195}Pt\{^{1}H\}$-NMR (CD_3NO_2): $\delta = (\nu_{1/2})$ triplet at -4353 ppm ($^{1}J(^{195}Pt-^{31}P) = 3511$ Hz). $^{31}P\{^{1}H\}$-NMR (CD_3NO_2): δ = singlet at 15.09, ^{195}Pt satellite doublet at 29.49 and $+0.68$ ppm ($^{1}J(^{195}Pt-^{31}P) = 3499$ Hz). A reversible Fe(II)/Fe(III) couple is observed at an $E_{1/2}$ value of $+721$ mV versus Fc/Fc^+, and the peak to peak separation (ΔE) was 67 mV. A broad, irreversible reduction wave is observed at -1454 mV versus Fc/Fc^+.

4.3.2. Preparation of $[Pd(9S3)(dppf)](PF_6)_2\cdot CH_3NO_2$

A mixture of $[Pd(dppf)Cl_2\cdot CH_2Cl_2]$ (279 mg, 0.345 mmol) and 9S3 (30 g, 0.166 mmol) was refluxed in 10 ml of CH_3OH for 1 h. The resulting deep purple solution was allowed to cool slightly before NH_4PF_6 (56.0 mg, 0.345 mmol) was added, and the mixture was refluxed for an additional 30 min. The solution was cooled in an ice bath to yield a deep purple–brown solid. The crystals were washed with CH_3OH (3×10 ml) and ether (3×10 ml). The initial product was then recrystallized from nitromethane–ether to yield dark brown crystals of $[Pd(9S3)(dppf)](PF_6)_2\cdot CH_3NO_2$ (117 mg, 55%) suitable for X-ray diffraction. Anal. Found: C, 41.37; H, 3.63; S, 8.17. Calc. for $C_{41}H_{43}F_{12}NO_2P_4PdFeS_3$: C, 41.31; H, 3.64; S, 8.07. The electronic absorption spectrum measured in MeCN showed three transitions with the first λ_{max} at 483 nm ($\varepsilon = 1810$), the second λ_{max} at 360 nm ($\varepsilon = 4840$), and the third λ_{max} at 275 nm ($\varepsilon = 68\,800$). FTIR (KBr, cm^{-1}): 3070, 3066, 3058, 3045, 2991, 2954, 2917, 1438, 1300, 1168, 1089, 1010, 853 (s, PF_6^-), 746, 708, 577, 501. ^{1}H-NMR (CD_3NO_2): δ = Ph: 7.89–7.66 (broad, 20H); Cp: singlets at 4.82 (4 H) and 4.72 (4 H); 9S3: complex AA′BB′ pattern centered at 2.91 (6H) and 2.48 (6H). $^{13}C\{^{1}H\}$-NMR (CD_3NO_2): δ = Ph: multiplets at 135.5 and 131.1 (16C), singlet at 134.9 (4C), doublet at 131.7 (4 C,

$^1J(^{13}C-^{31}P) = 10$ Hz); Cp: multiplets at 79.2 ppm (4H) and 77.3 (4H) ppm, doublet at 71.9 (2C, $^1J(^{13}C-^{31}P) =$ 67 Hz); 9S3: singlet at 35.9 (6C). $^{31}P\{^1H\}$-NMR (CD_3NO_2): $\delta =$ singlet at -0.47 ppm. A reversible oxidation wave, assigned as the Fe(II)/Fe(III) couple, is observed at an $E_{1/2}$ value of $+732$ mV versus Fc/Fc^+. The peak-to-peak separation (ΔE) was 69 mV. A sharp, irreversible reduction is observed at -880 mV versus Fc/Fc^+, and a second broad, poorly defined irreversible reduction wave is observed at -1476 mV versus Fc/Fc^+.

4.3.3. Preparation of [Ni(dppf)Cl_2]

A sample of $NiCl_2 \cdot 6H_2O$ (54.2 mg, 0.228 mmol) was heated to boiling in 10 ml of a mixture of 2-propanol/CH_3OH (v/v 5:2). A solution of dppf (111 mg, 0.200 mmol) in 10.0 ml of hot 2-propanol was added to the hot nickel solution, and the turbid green solution refluxed for 30 min. The solution was cooled in an ice bath, and green crystals of [Ni(dppf)Cl_2] (83.1 mg, 60.7%) were filtered, washed with cold CH_3OH (2×10 ml) and ether (2×10 ml). FTIR (KBr, cm^{-1}): 3074, 3070, 3062, 3049, 1442, 1310, 1168, 1089, 1010, 853, 746, 708, 577, 498, 475. $\mu_{eff} = 2.87$ BM.

4.4. X-ray structural analysis

4.4.1. [Pt(9S3)(dppf)]$(PF_6)_2 \cdot CH_3NO_2$

The crystal having approximate dimensions of $0.10 \times 0.27 \times 0.20$ mm, was mounted on a glass fiber. All measurements were made on a Siemens SMART 1K CCD diffractometer with graphite-monochromated Mo–K_α radiation ($\lambda = 0.71073$ Å). The absorption program SADABS (Sheldrick) was used for absorption correction [40]. The limiting indices were: $-13 \leq h \leq 14$, $-17 \leq k \leq 19$, $-38 \leq l \leq 33$. The refinement method used was a full-matrix least-squares on F^2. Hydrogen positions were calculated using ideal geometry and the C–H bond distances were fixed at 0.96 Å. The hydrogens were allowed to ride on the carbon during refinement. The extinction coefficient is 0.00080(4). Peaks on the final difference map ranged from -1.368 to 1.474 $e^- Å^{-3}$. Structure solution, refinement and the calculation of derived results were performed with the SHELXTL 5.03 package of computer programs [41].

4.4.2. [Pd(9S3)(dppf)]$(PF_6)_2 \cdot CH_3NO_2$

The crystal having approximate dimensions of $0.44 \times 0.27 \times 0.24$ mm, was mounted on a glass fiber. All measurements were made on a Siemens SMART 1K CCD diffractometer with graphite-monochromated Mo–K_α radiation ($\lambda = 0.71073$ Å). The absorption program SADABS (Sheldrick) was used for absorption correction [40]. The limiting indices were: $-11 \leq h \leq 14$, $-19 \leq k \leq 18$, $-38 \leq l \leq 30$. The refinement method used was a full-matrix least-squares on F^2. Hydrogen positions were calculated using ideal geometry and the C–H bond distances were fixed at 0.96 Å. The hydrogens were allowed to ride on the carbon during refinement. The extinction coefficient is 0.00041(5). Peaks on the final difference map ranged from -0.365 to 0.471 $e^- Å^{-3}$. Structure solution, refinement and the calculation of derived results were performed with the SHELXTL 5.03 package of computer programs [41].

5. Supplementary material

Crystallographic data for the structural analysis have been deposited with the Cambridge Crystallographic Data Centre, CCDC no. 159520 and 159521. Copies of this information may be obtained free of charge from The Director, CCDC, 12 Union Road, Cambridge CB2 1EZ, UK (Fax: +44-1223-336033; e-mail: deposit@ccdc.cam.ac.uk or www: http://www.ccdc.cam.ac.uk).

Acknowledgements

This research was generously supported by grants from the Wheeler Odor Research Center at UTC, the Research Corporation, the Petroleum Research Fund, and the Grote Chemistry Fund at UTC. We also appreciate the assistance of UTC students David F. Galas (NMR) and Pavle Repovic (electrochemistry) with some of the measurements on the Pt(II) complex.

References

[1] Heteroleptic platinum(II) complexes with crown thioether and phosphine ligands II: For Part I: see G.J. Grant, I.M. Poullaos, D.G. Galas, D.G. VanDerveer, J.D. Zubkowski, E.J. Valente, Inorg. Chem. 40 (2001) 564.
[2] A.J. Blake, M. Schröder, in: A.G. Sykes (Ed.), Advances in Inorganic Chemistry, vol. 35, Academic Press, New York, 1990, p. 2.
[3] S.R. Cooper, Acc. Chem. Res. 21 (1988) 141.
[4] S.R. Cooper, S.C. Rawle, Struct. Bonding (Berlin) 72 (1990) 1.
[5] M. Schröder, Pure Appl. Chem. 60 (1988) 517.
[6] S.G. Murray, F.R. Hartley, Chem. Rev. 8 (1981) 365.
[7] W.N. Setzer, E.L. Cacioppo, Q. Guo, G.J. Grant, D.D. Kim, J.L. Hubbard, D.G. VanDerveer, Inorg. Chem. 29 (1990) 2672.
[8] (a) R.D. Adams, S.B. Falloon, K.T. McBride, J.H. Yamamoto, Organometallics 14 (1995) 1739;
(b) R.D. Adams, J.H. Yamamoto, Organometallics 14 (1995) 3704.
[9] (a) A.J. Blake, A.J. Holder, T.I. Hyde, Y.V. Roberts, A.J. Lavery, M. Schröder, J. Organomet. Chem. 323 (1987) 261;
(b) A.J. Blake, A.J. Holder, T.I. Hyde, M. Schröder, J. Chem. Soc. Chem. Commun. (1987) 987.
[10] A.J. Blake, R.O. Gould, A.J. Holder, T.I. Hyde, A.J. Lavery, M.O. Odulate, M. Schröder, J. Chem. Soc. Chem. Commun. (1987) 118.
[11] A.J. Blake, R.O. Gould, A.J. Lavery, M. Schröder, Angew. Chem. Int. Ed. Engl. 25 (1986) 274.

[12] G.J. Grant, K.A. Sanders, W.N. Setzer, D.G. VanDerveer, Inorg. Chem. 30 (1991) 4053.
[13] S. Chandrasekhar, A. McAuley, Inorg. Chem. 31 (1992) 2663.
[14] A.J. Blake, R.D. Crofts, M. Schröder, J. Chem. Soc. Dalton Trans. (1993) 2259.
[15] (a) S.R. Cooper, S.C. Rawle, R. Yagbasan, D.J. Watkin, J. Am. Chem. Soc. 113 (1991) 1600;
(b) S.C. Rawle, R. Yagbasan, K. Prout, S.R. Cooper, J. Am. Chem. Soc. 1093 (1987) 6181;
(c) A.J. Blake, R.O. Gould, A.J. Holder, T.I. Hyde, M. Schröder, J. Chem. Soc. Dalton Trans. (1988) 1861.
[16] (a) M.N. Bell, A.J. Blake, R.O. Gould, A.J. Holder, T.I. Hyde, M. Schröder, J. Chem. Soc. Dalton Trans. (1990) 3841;
(b) M.N. Bell, A.J. Blake, M. Schröder, H.-J. Küppers, K. Wieghardt, Angew. Chem. Int. Ed. Engl. 26 (1987) 250;
(c) S.C. Rawle, T.J. Sewell, S.R. Cooper, Inorg. Chem. 26 (1987) 3769.
[17] (a) M.N. Bell, A.J. Blake, R.M. Christie, R.O. Gould, A.J. Holder, T.I. Hyde, M. Schröder, L.J. Yellowlees, J. Chem. Soc. Dalton Trans. (1992) 2977;
(b) A.J. Blake, R.O. Gould, A.J. Holder, T.I. Hyde, G. Reid, M. Schröder, J. Chem. Soc. Dalton Trans. (1990) 1759.
[18] G.J. Grant, N.S. Spangler, W.N. Setzer, D.G. VanDerveer, Inorg. Chim. Acta 246 (1996) 41.
[19] G.J. Grant, D.F. Galas, M.W. Jones, K.D. Loveday, W.T. Pennington, G.S. Schimek, C.T. Eagle, D.G. VanDerveer, Inorg. Chem. 37 (1998) 5299.
[20] T.W. Hambley, Inorg. Chem. 37 (1998) 3767.
[21] H. Nikol, H.-B. Bürgi, K.I. Hardcastle, H.B. Gray, Inorg. Chem. 34 (1995) 6319.
[22] For an elegant and very recent review covering the structural aspects of dppf metal complexes, see: G. Bandoli, A. Dolmella, Coord. Chem. Rev. 299 (2000) 161.
[23] H.-J. Kim, N.-S. Choi, S.W. Lee, J. Organomet. Chem. 616 (2000) 67.
[24] J. Granifo, M.E. Vargas, M.T. Garland, R. Baggio, Inorg. Chim. Acta 305 (2000) 143.
[25] G.Y. Zhen, D.P. Rillema, J.H. Reibenspies, Inorg. Chem. 38 (1999) 794.
[26] U. Casellato, D. Ajó, G. Valle, B. Corain, B. Longato, R. Graziani, J. Crystallogr. Spectrosc. Res. 18 (1988) 583.
[27] A.L. Balch, in: L.H. Pignolet (Ed.), Homogenous Catalysis with Metal Phosphine Complexes, Plenum, New York, 1983, pp. 167–213.
[28] P. Dierkes, P.W.N.M. van Leeuwen, J. Chem. Soc. Dalton Trans. (1999) 1520.
[29] A.J. Blake, Y.V. Roberts, M. Schröder, J. Chem. Soc. Dalton Trans. (1996) 1885.
[30] P.S. Pregosin, in: P.S. Pregosin (Ed.), Transition Metal Nuclear Magnetic Resonance, Elsevier, New York, 1991, p. 251 (and references cited therein).
[31] G.J. Grant, C.G. Brandow, D.F. Galas, J.P. Davis, W.P. Pennington, E.J. Valente, J.D. Zubkowski, J. Chem. Soc. Polyhedron (2001), submitted for publication. The complex is prepared by a direct combination of platinum(II) chloride and 9S3.
[32] A.J. Blake, A.J. Holder, Y.V. Roberts, M. Schröder, Acta Crystallogr. Sect. C 44 (1988) 360.
[33] The crystal structure for [Ni(dppf)]Cl_2] was published in Ref. [26], but to our knowledge the synthesis of the complex has not been described. We have included a brief synthesis in Section 4. The compound has just become commercially available from Aldrich chemical company.
[34] A.J. Blake, R.O. Gould, M.A. Halcrow, M. Schröder, J. Chem. Soc. Dalton Trans. (1993) 2909.
[35] (a) M.A. Bennett, J.K. Felixberger, A.C. Willis, Gazz. Chim. Ital. 123 (1993) 405;
(b) M.A. Bennett, A.J. Canty, J.K. Felixberger, L.M. Rendina, C. Sunderland, A.C. Willis, Inorg. Chem. 32 (1993) 1951.
[36] E.W. Abel, P.D. Beer, I. Moss, K.G. Orrell, V. Sik, P.A. Bates, M.B. Hurthouse, J. Chem. Soc. Chem. Commun. (1987) 978.
[37] For some other recent examples see: (a) S.-W.A. Fong, J.J. Vittal, T.S.A. Hor, Organometallics 19 (2000) 1427; (b) D.C. Smith Jr., C.M. Haar, E.D. Stevens, S.P. Nolan, W.J. Marshall, K.G. Moloy, Organometallics 19 (2000) 918; (c) A.R. Elsagir, F. Gassner, H. Gorls, E. Dinjus, J. Organomet. Chem 597 (2000) 139; (d) R. Pastorek, Z. Travnicek, J. Marek, D. Dastych, Z. Sindelar, Polyhedron 19 (2000) 1713.
[38] The sum of the van der Waals radii for platinum and sulfur is 3.50 Å: J.E. Huheey, E.A. Keiter, R.L. Keiter, Inorganic Chemistry, 4th ed., Harper Collins, New York, 1993, p. 292.
[39] From Ref. [22]: The parameter τ is defined as the mean dihedral angle between the two carbons on each Cp ring bonded to the P atoms and the centroid of the two Cp rings. The parameter measures the relative twist of the Cp(centroid)–Fe–Cp(centroid) axis.
[40] SADBAS: R.H. Blessing, Acta Crystallogr. Sect. A 51 (1995) 33.
[41] SHELXTL 5.03: Siemens, Siemens Analytical X-ray Instruments Inc., Madison, WI, USA, 1995.